



## ON THE HYDRODYNAMICAL DEVELOPMENT LENGTH FOR PRESSURE-DRIVEN PULSATING LAMINAR FLOW IN A PIPE

Orhan AYDIN and Cemalettin AYGÜN

Department of Mechanical Engineering Karadeniz Technical University  
61080 Trabzon, TURKEY, [oaydin@ktu.edu.tr](mailto:oaydin@ktu.edu.tr), [caygun@ktu.edu.tr](mailto:caygun@ktu.edu.tr)

(Geliş Tarihi: 10.09.2012 Kabul Tarihi: 05.02.2013)

**Abstract:** In this study, pulsating laminar flow in a pipe is considered numerically. The focus is concentrated on the hydrodynamical development length. At first, steady flow in a pipe is examined and a new correlation for the hydrodynamical development length is developed based on the scale analysis. Then, the pressure-driven pulsating flow is studied. For a constant value of Reynolds number, the effect of the frequency,  $F$  and the amplitude,  $A$  of the pulsating flow on the development length are determined. It is shown that  $F$  for its range of  $1 \leq F \leq 10$  dramatically affects the hydrodynamical development length while this effect becomes negligible either for very high values of  $F$  ( $F \geq 100$ ) or for low values of  $F$  ( $F \leq 0.1$ ). It is also disclosed that the amplitude,  $A$ , has a considerable effect on the entrance length for lower values of  $F$  ( $F \leq 0.1$ ). For some specific cases, results obtained are compared with those available in the open literature and a good agreement is obtained.

**Keywords:** Pulsating flow, pressure-driven, hydrodynamic development length, frequency, amplitude

## BİR BORU İÇERİSİNDE BASINÇ KAYNAKLI ATIMLI AKIŞ İÇİN HİDRODİNAMİK GELİŞME UZUNLUĞU

**Özet:** Bu çalışmada, bir boru içerisindeki atımlı akış sayısal olarak incelenmiştir. Çalışmanın ilgi odağı, hidrodinamik gelişme uzunluğudur. Öncelikle, bir boru içerisindeki daimi akış incelenmiş ve hidrodinamik gelişme uzunluğu için skala analizine dayalı yeni bir korelasyon geliştirilmiştir. Daha sonra, basınç kaynaklı atımlı akış durumu çalışılmış; Reynolds sayısının sabit bir değeri için, atımlı akış frekans ( $F$ ) ve genliğinin ( $A$ ) gelişme uzunluğu üzerindeki etkisi belirlenmiştir.  $F$ 'in  $1 \leq F \leq 10$  aralığındaki değerleri için hidrodinamik gelişme uzunluğu üzerinde önemli bir etkiye sahipken,  $F$ 'in çok yüksek ( $F \geq 100$ ) veya düşük ( $F \leq 0.1$ ) değerleri için bu etkinin ihmal edilebilir seviyede olduğu görülmüştür. Ayrıca, genliğin de etkisi incelenmiş,  $F$ 'in düşük değerleri için ( $F \leq 0.1$ ), genlik etkisinin önemli olduğu görülmüştür. Bazı özel durumlar için elde edilen sonuçlar literatürde var olanlarla karşılaştırılmış ve iyi bir uyum elde edilmiştir.

**Anahtar kelimeler:** Atımlı akış, basınç kaynaklı, hidrodinamik gelişme uzunluğu, frekans, genlik

### NOMENCLATURE

$A$	dimensionless amplitude, $u_A/u_M$
$C_1, C_2$	coefficients in Eq. [8]
$D$	diameter [m]
$f, F$	dimensional [Hz] and dimensionless frequency, $r_0^2 f/\nu$
$F\tau$	dimensionless phase
$J_0$	zeroth order Bessel function of first kind
$L$	pipe length [m]
$L/D$	hydrodynamical development length
$n$	wave number
$\tilde{P}_{en}^*$	complex form of dimensionless pressure gradient
$r, r^*$	dimensional [m] and dimensionless radial coordinate, $r/r_0$
$r_0$	radius [m]
$Re$	Reynolds number based on the pipe diameter, $u_M D/\nu$

$t, \tau$	dimensional [s] and dimensionless time (period), $\nu t/r_0^2$
$u, U$	dimensional [m/s] and dimensionless velocity, $u/u_M$
$u_A$	dimensional velocity fluctuation amplitude [m/s]
$x, X$	dimensional [m] and dimensionless axial coordinate, $x/D$

### Greek symbols

$\mu$	dynamic viscosity [kg/ms]
$\nu$	kinematic viscosity [m <sup>2</sup> /s]
$\rho$	density [kg/m <sup>3</sup> ]
$\tau$	dimensionless time (period), $\nu t/r_0^2$
$\omega$	angular frequency, $2\pi f$

### Subscript

$c$	center
$A$	amplitude
$M$	cycle averaged mean

## Superscript

- ~ Complex conjugate  
\* dimensionless quantity

## INTRODUCTION

Pulsatile flow is a specific unsteady flow in which the resulting flow is composed of a mean component and a periodically varying time-dependent component. Research interest on this flow has been increasing due to its presence in some industrial applications and in biological flows such as blood flow.

When fluid enters a tube or a duct, a hydrodynamic boundary layer begins to develop on the wall of the tube or the duct. As a fluid flows downstream, the boundary layer on one wall begins to intercept the boundary layer from the opposite wall. At this axial location, a fully developed, i.e. non-varying, velocity profile is reached far downstream from the entrance. Beyond this location, the flow is called the hydrodynamically fully developed flow and, the region is called as the hydrodynamically fully developed flow region. The region up to this location is called as the hydrodynamic entrance region or the hydrodynamic development region. For a steady flow, many studies have appeared in the existing literature studying the length of the hydrodynamic entrance region, i.e. the hydrodynamic development length. Durst et al. (2005) reviewed the existing literature on the entrance length. They evaluated available correlations for the entrance length in terms of the Reynolds number and finally they proposed a new correlation. For time-dependent flows, there is a scarcity of data available on the entrance length. For an unsteady flow, Atabek and Chang (1961) analytically estimated the length of the hydrodynamic entrance region. He and Ku (1994) numerically studied the entrance length and they found that this length decreased with an increase in Womersly number. Krijger et al. (1991) numerically studied pulsating entry flow in a plane channel. In a very recent study, Ray et al. (2012) studied development length as functions of the mean Reynolds number, the amplitude of mass flow rate pulsation and the pulsation frequency in the moderate and high Reynolds number regimes.

In the present computational investigation, it is aimed at studying the hydrodynamic entrance length for a pulsating flow. The effects of the frequency and the amplitude of the pulsation on hydrodynamic development length are determined.

## ANALYSIS

### Mathematical Formulation

The axially symmetric flow in a pipe is considered. The flow is assumed to be unsteady, 2-D, incompressible and laminar with constant thermophysical properties. The problem geometry is shown in Fig. 1.

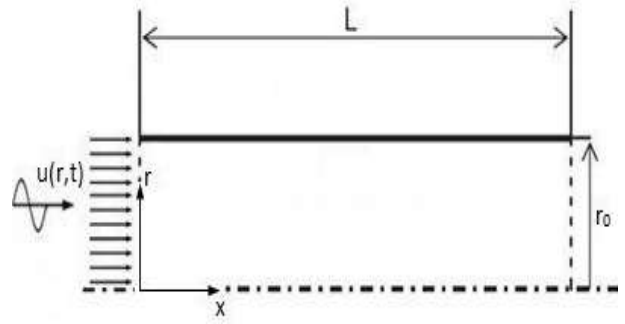


**Figure 1.** The geometry of the problem.

The partial differential equations governing the momentum transfer are the mass and momentum conservation equations. Considering the above assumptions, the most general form of the governing equations is given as follows:

$$\frac{\partial \rho \phi_k}{\partial t} + \frac{\partial}{\partial x_i} \left( \rho u_i \phi_k - \Gamma_k \frac{\partial \phi_k}{\partial x_i} \right) = S_{\phi_k} \quad k = 1, \dots, N \quad (1)$$

Here,  $\phi_k$  represents the general parameter, while  $\Gamma_k$  is the diffusion coefficient and  $S_{\phi_k}$  is the source term. Table 1 lists  $\phi_k$ ,  $\Gamma_k$  and  $S_{\phi_k}$  values for the conservations of mass and u-momentum equations.

**Table 1.** Diffusion coefficient and source terms

Equation	$\phi_k$	$\Gamma_k$	$S_{\phi_k}$
Continuity equation	1	-	-
u- momentum equation	$u$	$\mu$	$-\frac{\partial p}{\partial x}$

Boundary conditions are given as follows:

At the pipe inlet,

$$u(r,t) = u_0(r,t), \quad v = 0 \quad \text{at } x = 0 \quad (1)$$

where,  $u_0(r,t)$ , is constant for a uniform inlet flow, i.e.

$$u_0(t) = u_M \quad (2)$$

while it consists of two components for a pulsating flow:

$$u_0(t) = u_M + u_A \sin(2\pi fT) \quad (3)$$

At the pipe axis,

$$\frac{\partial u(r,t)}{\partial r} = 0 \quad \text{at } r = 0 \quad (4a)$$

At the pipe wall,

$$u(r,t)=0 \text{ at } r=r_0 \quad (4b)$$

The frequency-time domain of a sinusoid resulting from a pulsating flow is shown in Fig. 2. The sinusoid can be conceived of as existing a distance  $1/T$  out along the frequency axis and running parallel to the time axis. Consequently, when we speak about the behavior of the sinusoid in the time domain, we mean the projection of the curve onto the time plane (Chapra and Canale, 2005). Any point follows a sinusoid along the circle shown in the figure. When the point reaches its initial position, a cycle is completed. Here  $\tau$  represents the period, a constant, which is the time required for the point to reach its initial position.  $F$  represents the frequency that is the number of cycles per unit of time. The maximum value of the pulse gives us the amplitude.

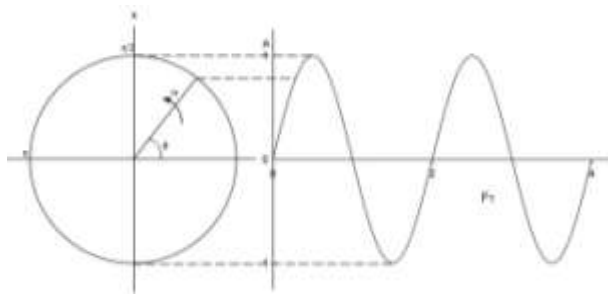


**Figure 2.** The frequency-time domain of a sinusoid resulting from a pulsating flow.

### Numerical Analysis

In the numerical study, the Fluent V6.1.22 CFD package (Fluent 6 User's Guide) based on the finite volume method is used to transform and solve these equations. The discretization scheme used is hybrid for the convective terms in the momentum equations, and the SIMPLE algorithm for pressure-velocity coupling. A user-defined function is introduced to the software for the pulsating inlet velocity profile. The mesh is generated in the Gambit 2.1.6 preprocessor (Gambit 2 User's Guide). Rectangular-type elements are used in the mesh generation. A non-uniform mesh structure is used in radial direction in order to capture very high gradients occurring near the wall while a uniform mesh structure is preferred in the axial direction. For any set of values of the governing parameters studied, mesh structure used is refined until the solution becomes grid-independent. The convergence factor was  $10^{-6}$  for each equation. For many test cases considered, a mesh size of  $320 \times 64$  nodes in the axial and radial directions is shown to be adequate since further refinement in mesh structure represents negligible changes in regarding parameters.

### Scale Analysis

A scale analysis is performed in order to predict the form of the entrance length correlation based on the driving mechanisms of the momentum transfer (Bejan, 1984; Arpacı and Larsen, 1984; Arpacı, 1997).

Scaling the mass conservation equation, we obtain

$$\frac{U_\infty}{X} \square \frac{U_\infty}{D} \quad (5)$$

which presents a balance between velocity gradients.

Similarly, the u-momentum equation can be scaled as in the following:

$$U_\infty \frac{U_\infty}{X}, U_\infty \frac{U_\infty}{D^2} \square \nu \frac{U_\infty}{D^2} \quad (6)$$

which presents a balance between inertia and viscous forces. From the above balances, we obtain

$$\text{Re} = \frac{U_\infty D}{\nu} \quad (7)$$

which implies the following correlation for the hydrodynamic entrance length:

$$\frac{L}{D} = \frac{C_1 \text{Re}}{1 + C_2 \text{Re}} \quad (8)$$

## RESULTS AND DISCUSSIONS

Here we consider a pipe with a length of 2 m and a diameter of 14 mm. On the choice of these values, an attention is paid to set  $L/D$  above the entrance length. The value of the Reynolds number is kept as constant 1000. The working fluid is air.

In this section, results are given for the steady flow and the pulsating flow in the following, respectively:

### Steady flow

In order to verify the numerical analysis followed, dimensionless velocity profile in the hydrodynamically fully developed region is obtained and shown in Fig. 3, which agrees fairly very well with the analytical solution. Figure 4 shows the dimensionless developing velocity profiles at different axial locations. The velocity profile at  $X=24$  coincides with that at the outlet the velocity profile is fully developed. The variation of the hydrodynamic entrance length with the Reynolds number is shown in Fig. 5. As expected, this length increases with an increase in  $\text{Re}$ . Some other results existing in the literature are also included in the figure. When the results obtained are fitted to the Eq. (5) derived by the scale analysis, the unknown coefficients  $C_1$  and  $C_2$  are obtained and the equation takes the following form:

$$\frac{L}{D} = \frac{0.055703 \text{Re}}{1 + 0.0000013 \text{Re}} \quad (9)$$

which is very elegant and in harmony with some data (Sparrow et al, 1964; Hornbeck, 1964; Vrentas et al, 1966) available in the literature. Since its form is constituted from the physics of the problem following a scale analysis, we hope it to be a reliable correlation in future studies and textbooks.

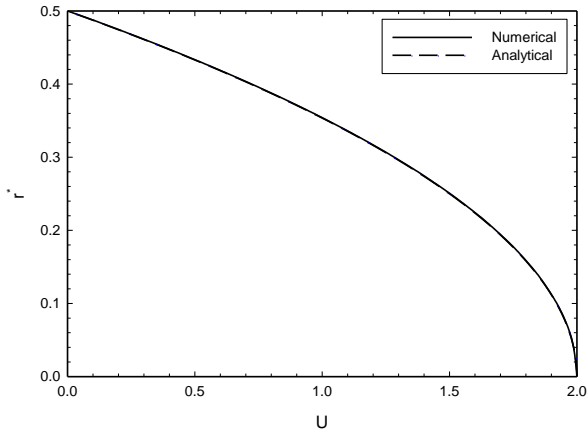


**Figure 3.** The dimensionless fully developed velocity profile.

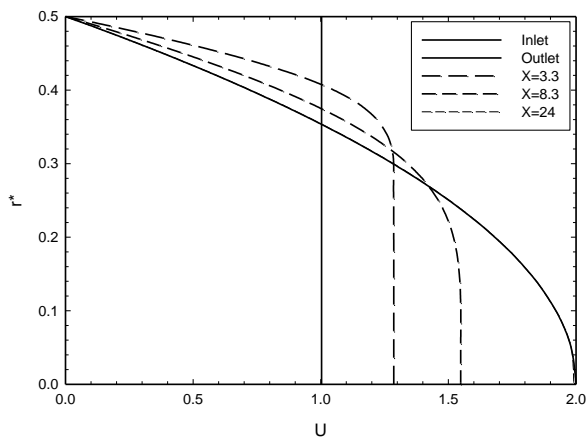


**Figure 4.** The dimensionless developing velocity profiles at different axial locations.

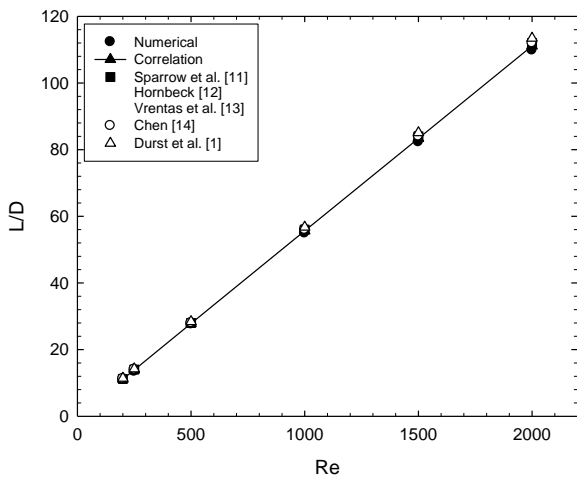


**Figure 5.** The variation of the hydrodynamic entrance length with the Reynolds number.

### Pulsating flow

At first, the numerical methodology followed is validated by comparing the results obtained with those available in the literature. For  $\alpha=12.5$  (Womersly number),  $A=1$  and  $Re=200$ , Fig. 6 shows dimensionless hydrodynamically fully developed velocity profile at  $\omega t=90$  and  $270$  (phase angle) which agrees fairly very well with the analytical solution given as follows (Uchida, 1956):

$$U^* = \frac{u}{u_M} = 2(1-r^{*2}) - \sum_{n=1}^{\infty} \frac{4\tilde{P}_{en}^* i}{\pi n F} \left[ 1 - \frac{J_0(\sqrt{2\pi n F i}^{3/2} r^*)}{J_0(\sqrt{2\pi n F i}^{3/2})} \right] e^{2\pi n F \tau i} \quad (10)$$

As seen from Fig. 6, there also exists an excellent harmony among our numerical results and numerical results by He and Ku (1994).

Figures 7 and 8 illustrate the hydrodynamic length,  $L/D$  and the centerline velocity,  $U_c$  with  $F\tau$  for various values of  $F$  at  $Re=1000$  and  $A=0.1, 0.5$  and  $0.95$ . As seen from Fig. 7, either for very high values of  $F$  (100 and 1000) or for very low values of  $F$  (0.1 and 0.01), the effect of  $F$  on  $L/D$  is negligible. This figure also shows that the entrance length is also affected strongly by the phase angle. With an increase in the frequency, the value of the phase angle at which the maximum value of the entrance length is attained shifts to higher values.

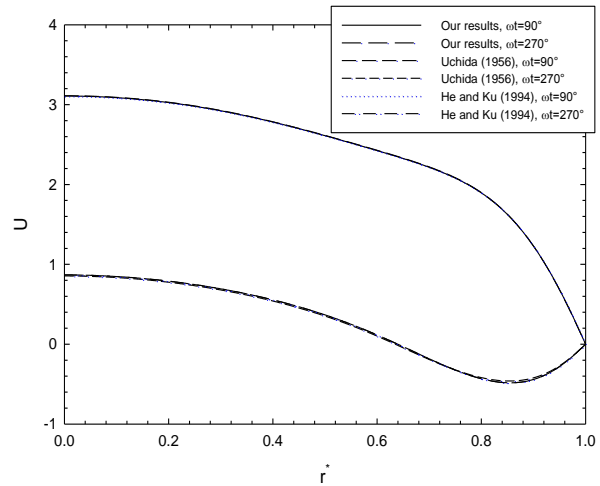


**Figure 6.** The dimensionless velocity profile at  $\omega t=90^\circ$  and  $270^\circ$ .

For example, the maximum length is reached at the phase angle of  $90^\circ$  for  $F=0.01$  while it is at  $180^\circ$  for  $F=10$ . Therefore, deciding the length according to a specific angle can be misleading. It is suggested here that the entrance length should be defined as the maximum length obtained by considering all the values of the phase angle. For a more detailed view on variation of the flow field with the regarding

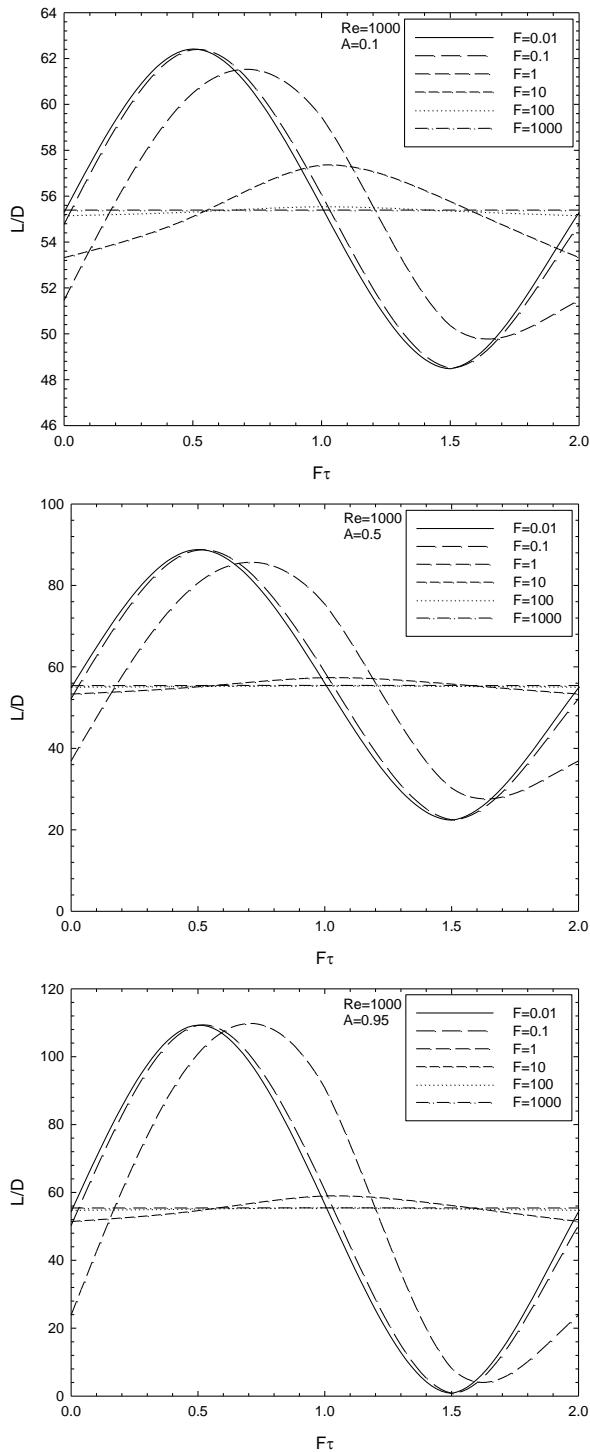


**Figure 7.** The hydrodynamic length,  $L/D$  with  $F\tau$  for various values of  $F$  at  $Re=1000$  and  $A=0.1, 0.5$  and  $0.95$ . parameters, the variation of the centerline velocity is also shown (see Fig. 8). Figure 9 illustrates the variation of the maximum entrance length with  $F$  for various values of  $A$ . For all the values of  $A$  considered, either for very high values of  $F$  ( $F \geq 100$ ) or for very low values of  $F$  ( $F \leq 0.1$ ), the influence of  $F$  on the entrance length is negligible. With an increase of  $F$  beyond  $0.1$  decreases the entrance length. The most dramatic decrease in the entrance length is observed in the range of  $1 \leq F \leq 10$ . The effect of the amplitude,  $A$  on the entrance length can also be observed from this figure.  $A$  has a considerable effect on the entrance length for

lower values of  $F$  ( $F \leq 0.1$ ). With an increase in  $F$  beyond  $F=0.1$ , the effect of  $A$  decreases and nearly diminishes for  $F \geq 100$ . For the phase angle of  $F\tau=0$  and  $0.5$ , the dimensionless velocity profiles at different axial locations at  $A=0.1, F=0.1$  and  $Re=1000$  are shown in Figs. 10 and 11, respectively. These figures well illustrate velocity fields at some specific axial stations, clearly describe their hydrodynamical development behavior and, in follows, the development length.

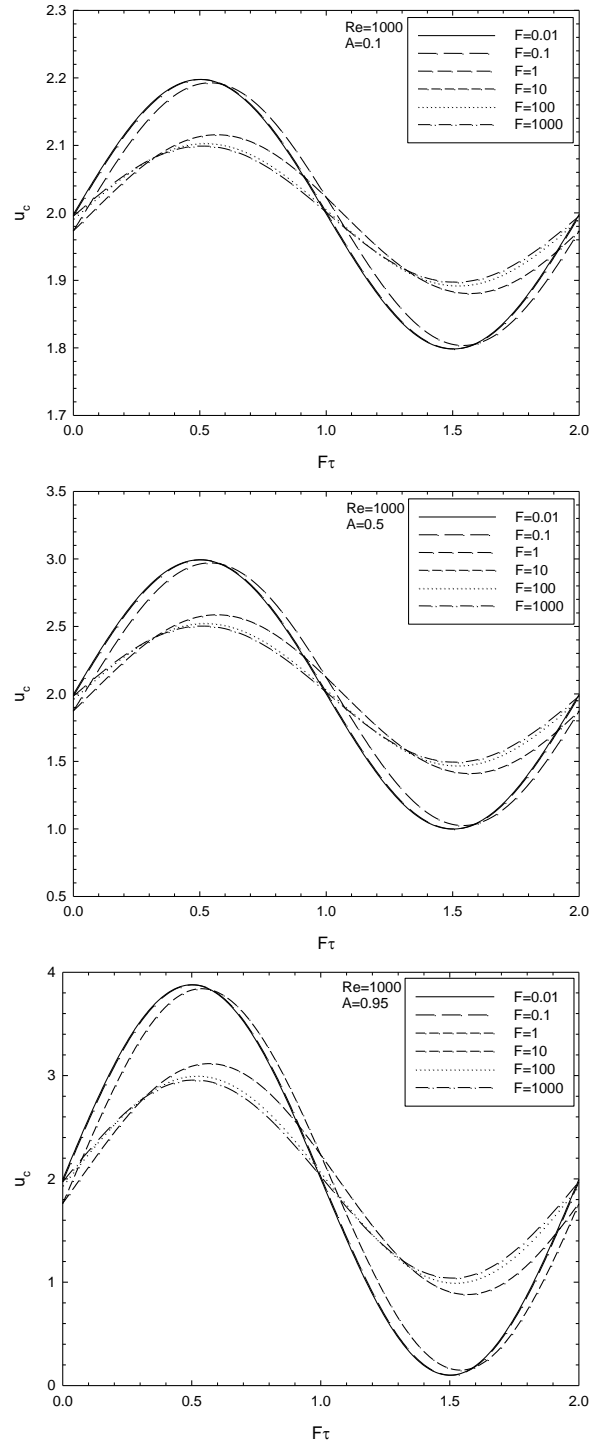


**Figure 8.** The centerline velocity,  $U_c$  with  $F\tau$  for various values of  $F$  at  $Re=1000$  and  $A=0.1, 0.5$  and  $0.95$ .

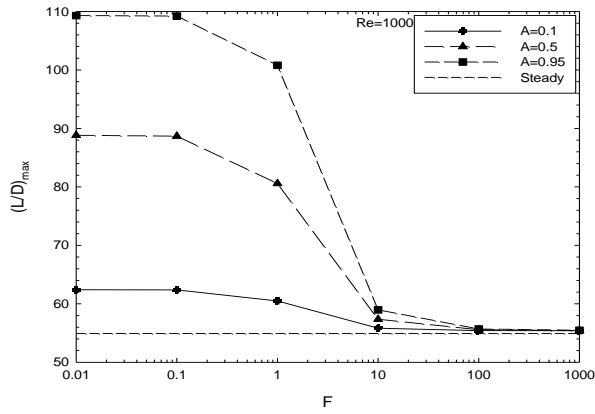


**Figure 9.** The variation of the maximum entrance length with  $F$  for various values of  $A$ .

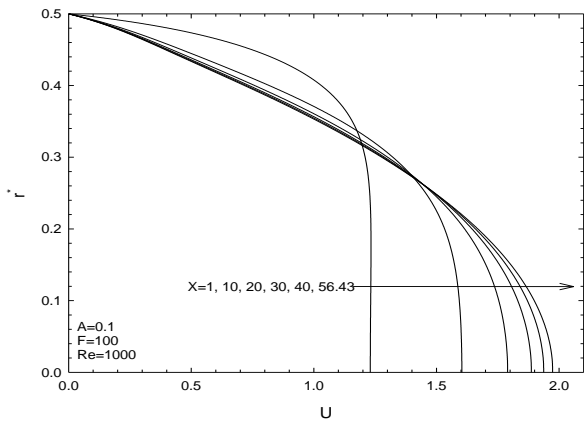
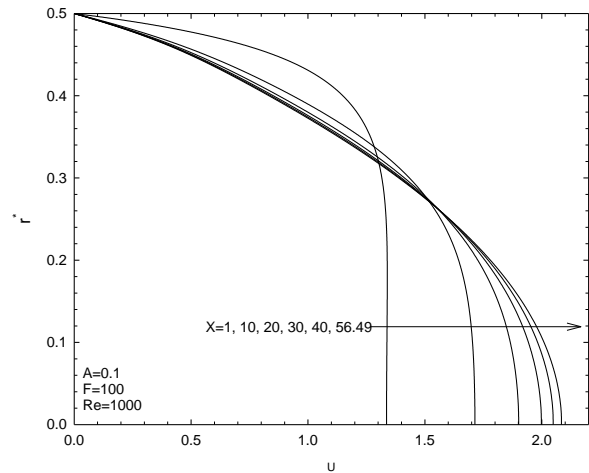
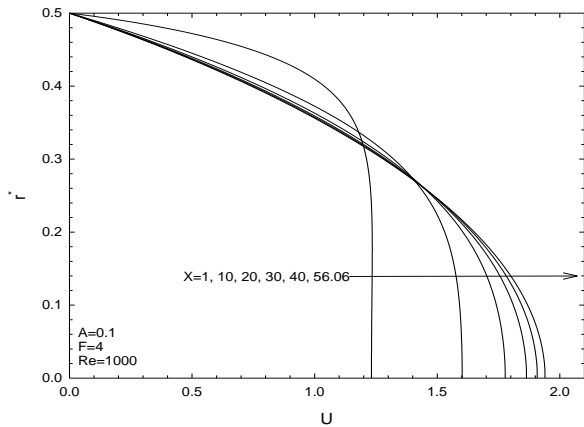
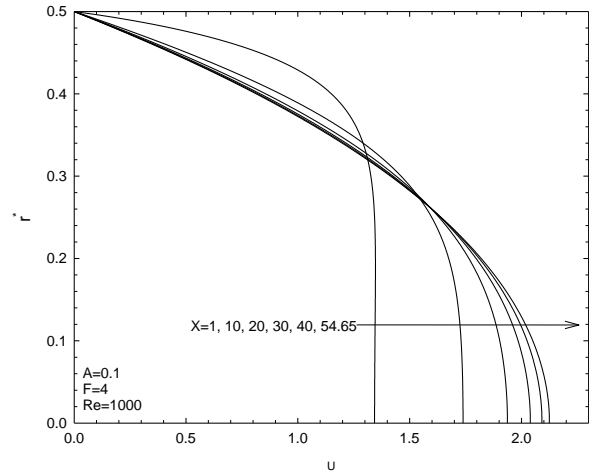
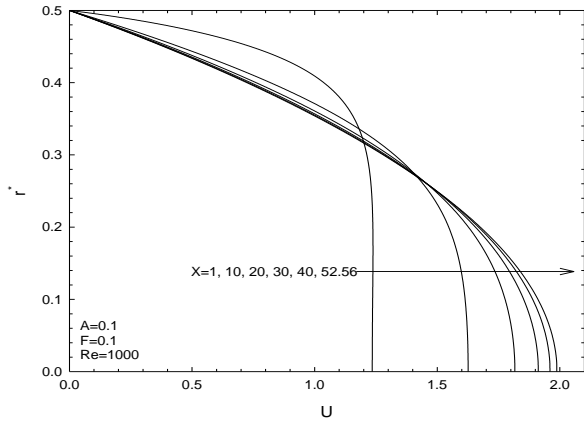
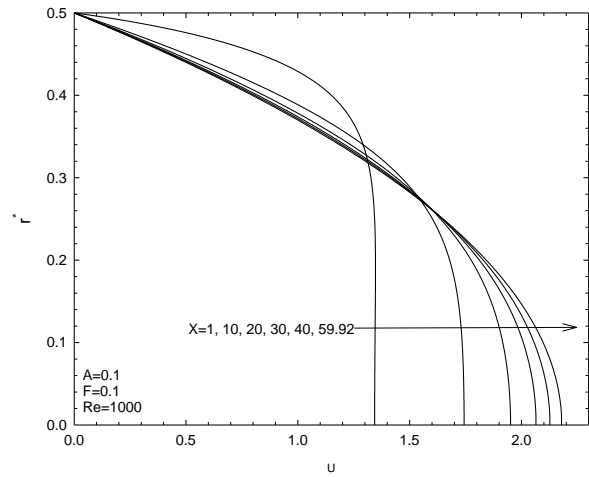


**Figure 10.** The dimensionless velocity profiles at different axial locations at  $A=0.1$ ,  $F=0.1$  and  $Re=1000$  for  $F\tau=0$ .

**Figure 11.** The dimensionless velocity profiles at different axial locations at  $A=0.1$ ,  $F=0.1$  and  $Re=1000$  for  $F\tau=0.5$ .

## CONCLUSIONS

The study has been focused on the hydrodynamical development length (i.e. the entrance length). At first, a new and useful correlation developed based on the scale analysis has been proposed for the hydrodynamical development length for the steady flow in pipes. The pulsating flow has been studied for a broad range of the frequency and the amplitude of the pulsating flow is studied at a constant value of Reynolds number. It is disclosed that the development length has been affected

dramatically by  $F$  in the range of  $1 \leq F \leq 10$  while this effect becomes negligible either for very high values of  $F$  ( $F \geq 100$ ) or for very low values of  $F$  ( $F \leq 0.1$ ). It is also disclosed that the amplitude,  $A$ , has a considerable effect on the entrance length for lower values of  $F$  ( $F \leq 0.1$ ). It is obtained that with an increase in  $F$  beyond  $F=0.1$ , the effect of  $A$  decreases and nearly diminishes for  $F \geq 100$ .

## ACKNOWLEDGMENT

The first author of this article is indebted to the Turkish Academy of Sciences (TUBA) for the financial support provided under the Programme to Reward Success Young Scientists (TUBA-GEBIT).

## REFERENCES

- Arpacı, V. S., *Microscales of Turbulence- Heat and Mass Transfer Correlations*, Gordon and Breach Sci. Pub., Amsterdam, 1997.
- Arpacı, V. S., and Larsen, P. S., *Convection Heat Transfer*. Prentice Hall, New Jersey, 1984.
- Atabek, H. B., and Chang, C. C., Oscillatory flow near the entry of a circular tube, *ZAMP*, 12, pp.185-201, 1961.
- Bejan, A., *Convection Heat Transfer*, John Wiley&Sons, New York, 1984.
- Chapra, S. C., and Canale, R. P., *Numerical Methods for Engineers*, McGraw-Hill, New York Science/Engineering, 2005, pp. 517-519, 2005.
- Chen, R.Y., Flow in the entrance region at low Reynolds numbers, *J. Fluids Eng.*, 95, pp.153-158, 1973.
- Durst, F., Ray, S., Ünsal, B., and Bayoumi, O. A., The development lengths of laminar pipe and channel flows, *J. Fluids Engineering*, 127, pp. 1154–1160, 2005.
- Fluent 6 User's Guide, Fluent Inc., Lebanon, Nh.
- Gambit 2 User's Guide, Fluent Inc., Lebanon, Nh.
- He, X., and Ku, D. N., Unsteady entrance flow development in a straight tube, *Journal of Biomechanical Engineering*, 116, pp. 355-360, 1994.
- Hornbeck, R. W., Laminar flow in the entrance region of a pipe, *Appl. Sci. Res. Sect. A*, 13, pp. 224-236, 1964.
- Krijger, J.K.B., Hillen, B., Hoogstraten, H.W., Pulsating entry-flow in a plane channel, *ZAMP*, 42, pp. 139–153, 1991.
- Ray, S., Ünsal, B., Durst, F., Development length of sinusoidally pulsating laminar pipe flows in moderate and high Reynolds number regimes, *Int. J. Heat Mass Transfer*, 37, pp. 167-176, 2012.
- Sparrow, E. M., Lin, S. H., and Lundgren, T. S., Flow development in the hydrodynamic entrance region of tubes and ducts, *Phys. Fluids*, 7(3), pp. 338-347, 1964.
- Uchida, S., The pulsating viscous flow superposed on the steady laminar motion of incompressible fluid in a circular pipe, *ZAMP*, 7, pp. 403–422, 1956.
- Vrentas, J.S., Duda, J.L., and Barger, K.G., Effect of axial diffusion of vorticity on flow development in circular conduits, *AIChE J.*, 12, pp. 837-844, 1966.